Journal of Power Sources, *33* (1991) 213–220

Influence of phosphoric acid on both the electrochemistry and the operating behaviour of the lead/acid system

J. Garche, H. Döring and **K. Wiesener**
Dresden University of Technology, Department of Chemistry, Mommenstrasse 13, O-8027 Dresden (F.R.G.)

Abstract

The addition of phosphoric acid to the electrolyte or the positive active material of the lead/acid battery yields different results. For antimony-free batteries, the capacity is reduced but the lifetime is improved under deep-discharge service. Both effects at the positive electrode appear to originate from the same cause, namely, the crystal size of $PbSO_4$ is decreased considerably in the presence of phosphoric acid. The utilization of the positive active material is reduced because the resulting fine-grained $PbSO_4$ covers the PbO_2. On the other hand, the $PbSO_4$ protects the corrosion layer against further discharge. The action of phosphoric acid is demonstrated through cyclic voltammetric, potential-step, impedance and microscopic investigations.

Introduction

Additions of phosphoric acid, or its salts, either to the electrolyte or to the positive active material of the lead/acid battery have been used for about 100 years [1–7]. These additives are aimed at increasing the lifetime of the battery. Many other effects have, however, also been observed, e.g., capacity loss. Since the introduction of lead–calcium alloys in lead/acid battery designs, the practical importance of phosphoric acid addition has increased because of the resulting improvement in the charge behaviour of batteries with non-antimonial grids. The mechanism of the manifold action of phosphoric acid is not fully understood, despite systematic studies since about 1930 [8–16]. This paper presents a model for the action of phosphoric acid in the lead/acid system and attempts to explain empirical observations when using this additive.

Influence of phosphoric acid on lead/acid electrochemistry

Addition of phosphoric acid (H_3PO_4) to sulphuric acid changes the features of the cyclic voltammogram (i.e., the dynamic current–potential curve) of the lead electrode [17]. The changes are normally observed only at potentials above +500 mV (note, all potentials are given with respect to a

0378-7753/91/$3.50

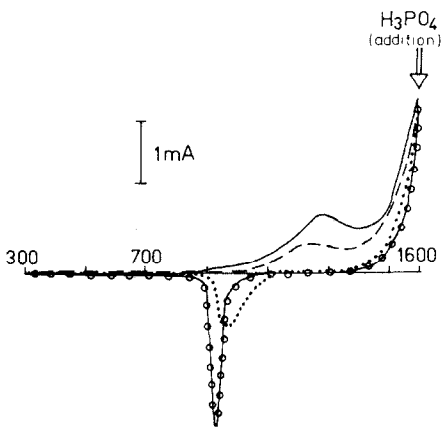

Fig. 1. Voltammograms for a pre-polarized lead electrode (+1600 mV, 15 min) in 0.85 M H_2SO_4; sweep rate 10 mV s^{-1}. (———) Without H_3PO_4. With 2.5×10^{-2} M H_3PO_4, (○○○○) first reduction cycle 1600 mV → 300 mV, (– – – –) oxidation cycle 300 mV → 1600 mV, (· · · · ·) second reduction cycle 1600 mV → 300 mV.

Hg/$HgSO_4$ reference electrode). Therefore, phosphoric acid should influence only the positive electrode of a lead/acid cell.

The phosphoric acid acts only during the oxidation process, as the voltammograms for a lead electrode show (Fig. 1). This electrode was oxidized in 0.85 M H_2SO_4 at +1600 mV for 15 min and then H_3PO_4 was added. The initial reduction process was not influenced by phosphoric acid. Only the subsequent oxidation was perturbed and then also the second reduction process. The same curves were obtained when the addition of phosphoric acid was effected after the first reduction process at a potential of +300 mV. This suggests that phosphoric acid influences the oxidation of $PbSO_4$ to PbO_2 but does not disturb the reduction of PbO_2, formed in pure sulphuric acid. Only the reduction of PbO_2, formed in the presence of phosphoric acid, is prevented. The reason for this is the specific adsorption of phosphoric acid on the electrode surface in the oxidation potential region, as described by Carr and Hampson [11]. Such specific adsorption is observed for sulphate ions as well, but the phosphoric acid adsorption is stronger, as demonstrated by impedance measurements [17].

The specific adsorption of phosphoric acid leads to an oversaturation of PbO_2 and to a change in the growth mechanism of PbO_2. The three-dimensional growth changes to a two-dimensional one, as proven by potential-step experiments [17]. Consequently, a fine grain structure of PbO_2 is built up. In the reduction process, this structure results in a fine grain structure of $PbSO_4$, see Fig. 2. During cycling, some coarse $PbSO_4$ crystals are formed on this structure at surface imperfections [16].

The nearly amorphous $PbSO_4$ covers the PbO_2 relatively fast and thus hinders further reduction. Only when the potential reaches the Pb/$PbSO_4$ region, is a reduction possible, as indicated by the strong reduction peak in the voltammogram at −950 mV after the tenth cycle (300 ⇌ 1600 mV), Fig. 3.

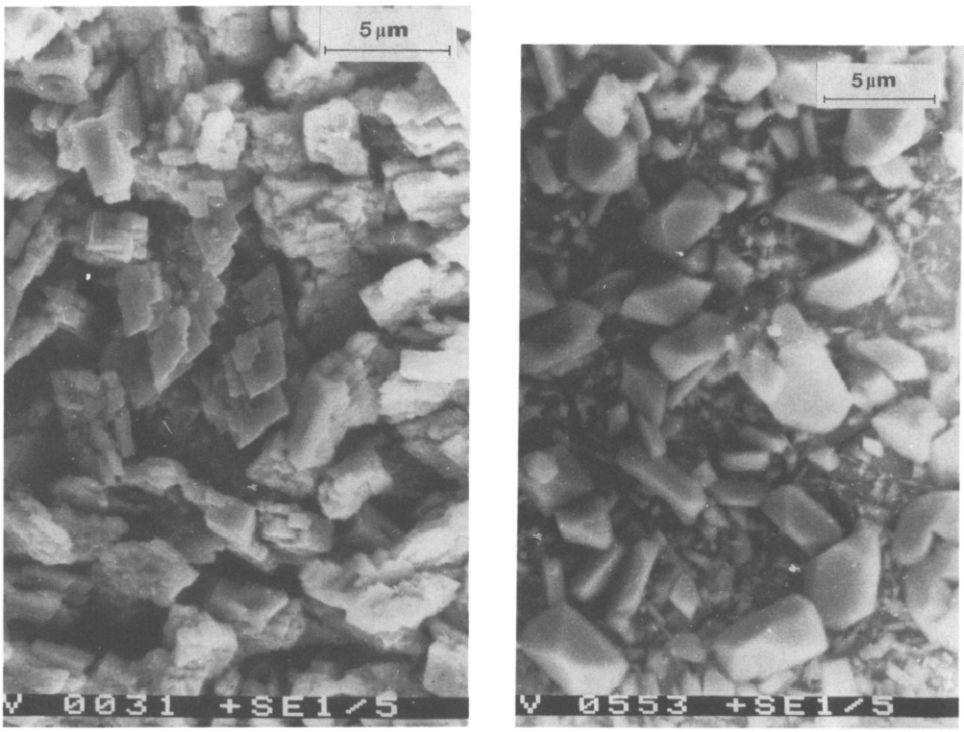

(a) (b)

Fig. 2. Influence of H_3PO_4 addition on particle morphology of a $PbO_2/PbSO_4$ electrode after 80 cycles (300 ⇌ 1600 mV): (a) 0.85 M H_2SO_4; (b) 0.85 M $H_2SO_4 + 2.5 \times 10^{-2}$ M H_3PO_4.

Under our measurement conditions (small Pb surface), no evidence could be found for the yellow, soluble Pb(IV) compound described by Bode and Voss [8, 9].

The phosphoric acid adsorption also leads to a decrease of the rate of oxygen evolution, as shown in Fig. 3 and Table 1.

It is well known that $PbSO_4$ layers act as semi-permeable membranes, blocking the transport of both sulphate and lead ions. Thus, the pH can increase under the layer and α-PbO_2 formation is favoured. The finer the $PbSO_4$, the poorer the permeability. This means that, in the presence of H_3PO_4, the α-PbO_2 content of the electrode increases. For example, the X-ray diffraction intensity relation $I(\beta\text{-}PbO_2)/I(\alpha\text{-}PbO_2)$ is reduced from 0.44 in 0.85 M H_2SO_4 to 0.22 in 0.85 M $H_2SO_4 + 2.5 \times 10^{-2}$ M H_3PO_4 at a lead electrode after 60 cycles (300 ⇌ 1600 mV).

Influence of phosphoric acid on lead/acid operation

The practical effects of H_3PO_4 additions on lead/acid battery performance are summarized in an excellent review by Voss [8] that is based on the

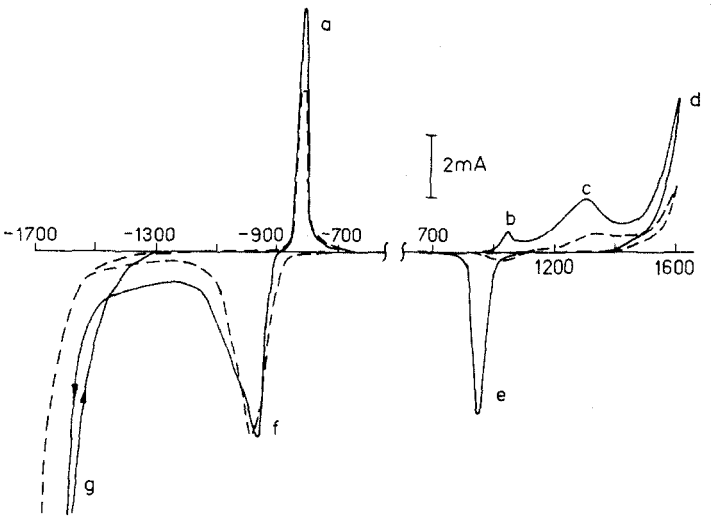

Fig. 3. Voltammogram for a lead electrode in 0.85 M H_2SO_4 with (– – –) and without (———) H_3PO_4 addition (2.5×10^{-2} M) after the 10th cycle (300 ⇌ 1600 mV); sweep rate 10 mV s^{-1}.

TABLE 1

Oxygen evolution at a lead electrode at different potentials after 20 h

Applied potential (mV)	Volume of oxygen (ml cm^{-2})	
	Without H_3PO_4	With H_3PO_4
+1550	5.4	2.8
+1500	1.7	0.7

unpublished results of Kugel and Rabl. We have slightly changed Voss's summary of those effects, as follows:

(i) improves the deep-discharge behaviour of lead/acid cells with antimony-free grids
(ii) increases the cycle lifetime of lead/acid cells
(iii) reduces the capacity of positive pasted electrodes
(iv) reduces self-discharge
(v) retards sulphatation on stand after deep discharge
(vi) reduces lead corrosion
(vii) reduces the shedding rate of the positive active material

Deep-discharge behaviour

PbO_2 is reduced to $PbSO_4$ during discharge of the positive electrode. PbO_2, however, is present not only in the active material but also in the

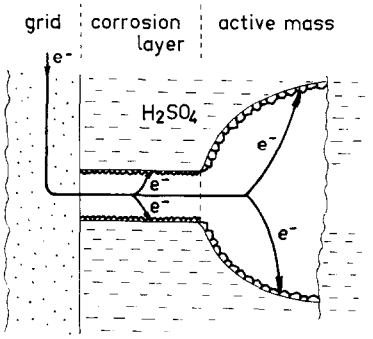

Fig. 4. Model for the electron transport through the positive electrode during discharge.

corrosion layer. This means that the PbO_2 in the corrosion layer should also be reduced. Nevertheless, $PbSO_4$ normally covers the PbO_2 and blocks further reduction of the corrosion-layer PbO_2. Consequently, up to the end of discharge of the electrode there is still an electronic pathway of PbO_2 in the corrosion layer to the active material (Fig. 4). During the next charge, the corrosion-layer $PbSO_4$ is again oxidized to PbO_2. However, during cycle lifetime, this behaviour can be changed if the cyrstal structure of $PbSO_4$ in the corrosion layer is too coarse. Such is the case at antimony-free grids: because the $PbSO_4$ is coarse, more PbO_2 in the corrosion layer is reduced, i.e., the electronic pathway is narrower. Moreover, during the next charge, not all the coarse $PbSO_4$ crystals are oxidized.

During the following cycles, the amount of non-oxidizable $PbSO_4$ increases and finally reaches a stage at which nearly all the PbO_2 is reduced on the next discharge. Under these conditions, the electronic pathway to the active material is blocked and antimony-free electrodes are no longer dischargeable (Fig. 5).

Addition of phosphoric acid to antimony-free electrodes reduces the crystal size of $PbSO_4$ (see Fig. 2). As a result, the further reduction of the corrosion layer PbO_2 is prevented, as fundamental experiments have shown (see Figs. 1 and 3), and the behaviour of the corrosion layer is antimony-like. Thus, there is an increase in the cycle lifetime, but only under deep-discharge conditions, as demonstrated by the data presented in Fig. 6.

Capacity loss of pasted electrodes

The fine grain structure of $PbSO_4$ (see Fig. 2), as a consequence of the phosphoric acid additions, acts not only in the corrosion layer but also in the active material and hinders discharge of the latter. This results in a loss in capacity, usually in the range of 15%.

Self-discharge

Self-discharge at the positive electrode is determined mainly by two processes [18]

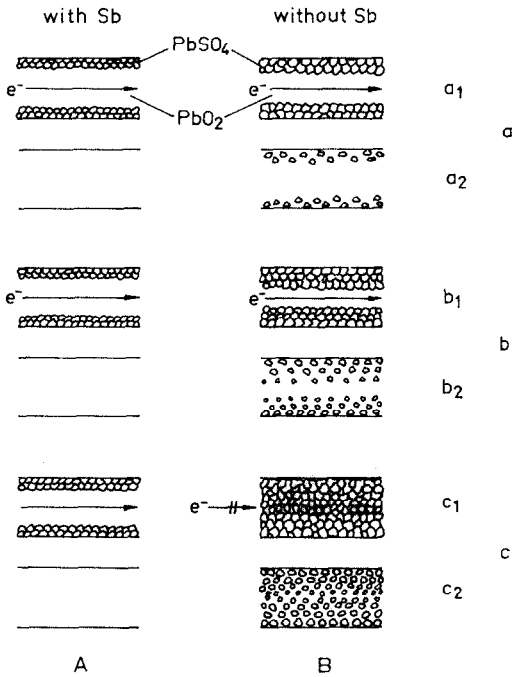

Fig. 5. Schematic of the composition of the corrosion layer at the end of discharge (a_1, b_1, c_1) and end of charge (a_2, b_2, c_2) and influence of grid material (A, with Sb; B, Sb-free) and cycle lifetime (a, first cycle; b, intermediate cycle; c, end of cycle lifetime).

$$PbO_2 + H_2SO_4 \rightarrow PbSO_4 + \tfrac{1}{2}O_2 + H_2O \quad (1)$$

$$PbO_2 + Pb + 2H_2SO_4 \rightarrow 2PbSO_4 + 2H_2O \quad (2)$$

The rate of reaction (1) is determined by both the concentration of sulphuric acid and the oxygen overvoltage at PbO_2. The latter increases in the presence of H_3PO_4 (see Fig. 1, Table 1 and ref. 19). Consequently, the rate of reaction (1) is decreased if H_3PO_4 is added.

The rate of reaction (2) is determined strongly by the structure of the corrosion layer and that of the $PbSO_4$, formed by the self-discharge reaction. Fine grain $PbSO_4$, as formed on H_3PO_4 additions, covers the lead grid. Thus, the surface area of the grid is decreased and, thereby, the reaction rate decreases.

Corrosion

The corrosion process, i.e., the oxidation of lead, is hindered by H_3PO_4 additions as is shown in Fig. 1. Consequently, the corrosion layer thickness is decreased [17].

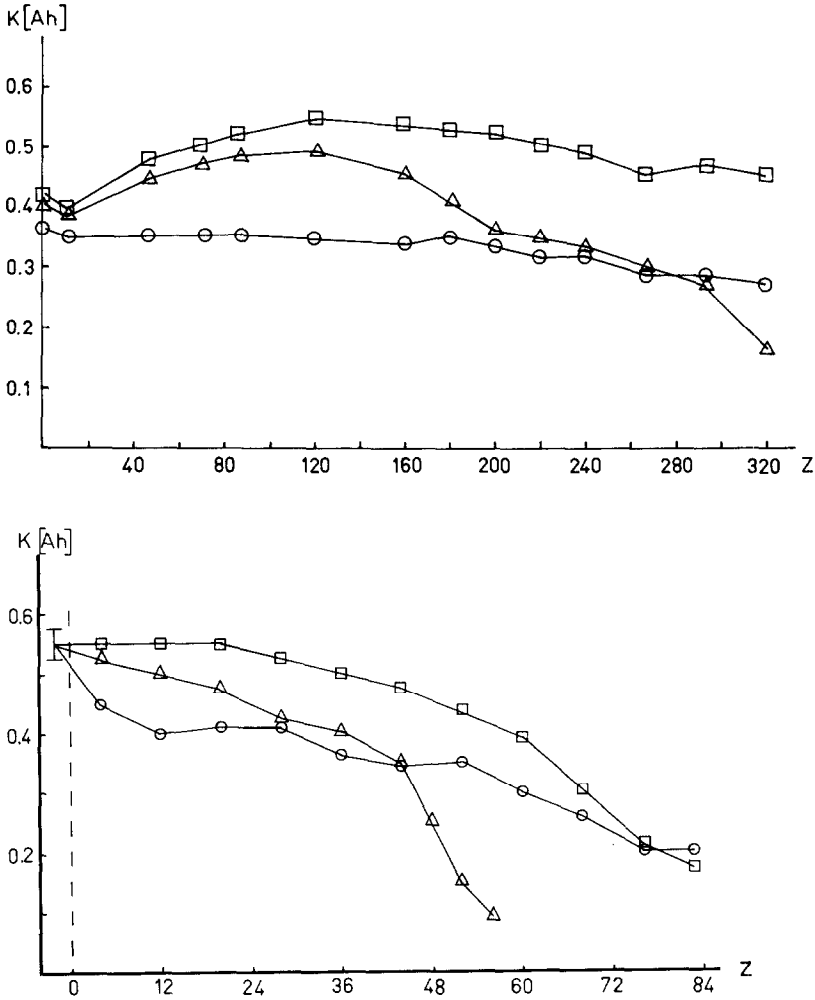

Fig. 6. Capacity as a function of cycle number, 0.5 A h electrode in H_2SO_4 ($\rho = 1.28$ g cm^{-2}) with 6 wt.% SiO_2. (a) 50% DOD, $I_{dis} \triangleq 0.17 \times C_{20}$; $I_{ch} \triangleq 0.064 \times C_{20}$; $F_{ch} \triangleq 1.13$; (b) 100% DOD, $I_{dis} \triangleq 0.1 \times C_{20}$; $I_{ch} \triangleq 0.12 \times C_{20}$; $F_{ch} \triangleq 1.2$. (-□-) Pb–2.5 wt.%Sb; (—△-) Pb; (-○-) Pb + 30×10^{-2} M H_3PO_4.

Sulphatation

Sulphatation in the deep-discharge state is prevented by H_3PO_4 additions because of the fine-grain $PbSO_4$ structure that is formed in the presence of phosphoric acid (Fig. 2).

Shedding

The shedding rate is dependent on the mechanical stability of the active material. The stability is increased by α-PbO_2. Upon addition of H_3PO_4, the

α-PbO_2 content grows. Therefore, the active material becomes harder and the rate of shedding is decreased.

References

1 W. A. Boese, *Ger. Patent 85 053* (1893).
2 C. Brault, *U.S. Patent 625 287* (1899).
3 F. D. Cheney, *U.S. Patent 1 385 305* (1921).
4 M. Kugel, *Ger. Patent 480 149* (1926).
5 K. Neumann, *Fr. Patent 690 409* (1930).
6 M. Kugel and M. Rabl, *Ger. Patent 516 173* (1930).
7 O. Jache, *Ger. Pat. 1 671 693* (1967).
8 E. Voss, *J. Power Sources, 24* (1988) 171.
9 H. Bode and E. Voss, *Electrochim. Acta, 6* (1962) 11.
10 S. Tudor, A. Weisstuch and S. H. Davang, *Electrochem. Technol., 3* (1965) 90; *4* (1966) 406; *5* (1967) 21.
11 J. P. Carr and N. A. Hampson, *J. Electroanal. Chem., 28* (1970) 65.
12 R. F. Amlie, E. Y. Weissmann, C. K. Morehouse and N. M. Qureshi, *J. Electrochem. Soc., 119* (1972) 568.
13 K. R. Bullock and D. H. McClelland, *J. Electrochem. Soc., 124* (1977) 1478.
14 K. Bullock, *J. Electrochem. Soc., 126* (1979) 360; *126* (1979) 1848.
15 B. K. Mahato, *J. Electrochem. Soc., 126* (1979) 366.
16 G. A. Morris, P. J. Mitchell, N. A. Hampson and J. I. Dyson, in T. Keily and B. W. Baxter (eds.), *Power Sources 12*, Int. Power Sources Symp. Committee, Leatherhead, U.K., 1989, pp. 61–75.
17 H. Döring, J. Garche and K. Wiesener, *J. Power Sources*, in press.
18 J. Garche, *J. Power Sources, 30* (1990) 47.
19 O. Z. Rasina, I. A. Aguf, M. A. Dassoyan, *Z. Prikl. Khim., 58* (1985) 1039.